Contribution of O$_2$ plasma treatment and amine modified GOs on film properties of conductive PEDOT:PSS: Application in indium tin oxide free solution processed blue OLED

Halide Diker[a], Fatih Yesil[b], Canan Varlikli[a,*]

[a] *Department of Photonics, Izmir Institute of Technology, 35430, Urla, Izmir, Turkey*
[b] *Solar Energy Institute, Ege University, 35100, Bornova, Izmir, Turkey*

ARTICLE INFO

ABSTRACT

Primary (n-propyl amine, n-PRYLA), secondary (dipropyl amine, DPRYLA) and alcohol (propanol amine, PRPOHA) amine derivatives were used as amine sources in graphene oxide (GO) modification and obtained samples were named as nPRYLA-GO, DPRYLA-GO and PRPOHA-GO, respectively. Modified graphene oxide (mGO) derivatives were doped in poly (3,4-ethylenedioxythiophene)-poly(styrenesulfonate) (PH1000) and O$_2$ plasma treatment (70W, 3 min) was applied on the spin casted films. PH1000:mGO films presented high optical transparency values (> 90%) and low resistivity (177–183 Ω/sq). The roughness values were increased especially when the hydrophobic alkyl chain containing DPRYLA-GO and nPRYLA-GO were doped in PH1000. Prepared films were utilized as anode in solution processed blue organic light emitting diode. PH1000:PRPOHA-GO anode presented more than 30 nm of decrement in full with at half maximum and 1.6, 1.5 and 1.9 fold enhancements in current, power and external quantum efficiency values, compared to those of ITO anode, respectively.

1. Introduction

Indium tin oxide (ITO) is the most commonly used TCO electrode in organic light emitting diodes (OLED). However, some critical drawbacks of ITO such as intrinsic brittleness, high cost and need for high vacuum and temperature for its production, motivate the researchers on developing alternative materials to replace it [1]. Conductive polymers [2,3], carbon nanotubes [4,5], graphene and its derivatives [6–8], metal nanowires [9] and grids [10] represent the widely investigated electrode materials. Excellent mechanical flexibility, low-cost and solution-processability of poly(3,4-ethylenedioxythiophene):poly (styrenesulfonate) (PEDOT:PSS) make it a predominant candidate to replace ITO [11,12].

The conductivity and dispersion stability of PEDOT:PSS in water depends on the PEDOT to PSS ratio. Although commercially available PH1000 (*PEDOT:PSS; 1:2.5*) is known as the high conductive grade PEDOT:PSS, it still needs enhancement in its conductivity and transparency to serve as an ITO alternative. The most commonly applied treatment method is the addition of high boiling solvents with high polarity (e.g. ethylene glycol "EG", dimethylsulfoxide "DMSO", dimethylformamide "DMF") into PH1000 [11–13]. Strong screening

effects of these solvents, those of which weaken the electrostatic interactions between the positively charged PEDOT and negatively charged PSS groups, results in a conformational change in PEDOT chains and thereby increase the conductivity of PH1000 films significantly [14]. The contribution of ionic liquids, anionic surfactants, co-solvents, acids, ultrasound and also some post-treatment methods on the conductivity enhancement were also reported by several groups [3,11,15–27]; for now, acid (especially H$_2$SO$_4$) treatment seems to take the field [3,21,22]. Recently, O$_2$ plasma treatment was introduced as an alternative procedure and without the aid of high polarity solvent and acid treatment, promising low resistivity values (36Ω/sq) were obtained. However, corresponding optical transparency values (73%) were rather low to be used in OLEDs [28]. Graphene derivatives of graphene oxide (GO) and/or reduced graphene oxide (rGO) have also been utilized as dopants in PH1000 and low surface resistivity (80–92 Ω/sq) and ITO compatible optical transparency values (80–92%) were reported [29–35]. The best optical transparency versus surface resistivity values reported in current literature those of which introduce H$_2$SO$_4$ or plasma treatment on PH1000 films and GO and/or rGO derivatives as dopants in PH1000 are summarized in Fig. 1.

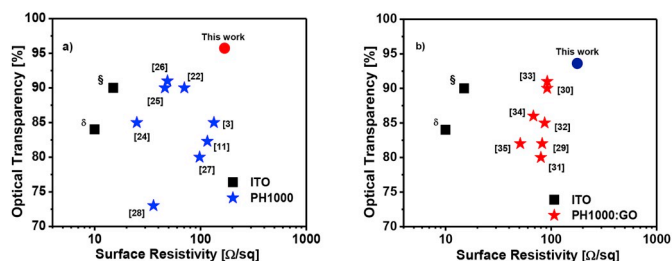In this manuscript, in addition to known thermal, solvent and H$_2$SO$_4$

Fig. 1. Optical transparency versus surface resistivity values of a) H_2SO_4 or O_2 plasma treated PH1000 films and b) GO and/or rGO derivatives doped in PH1000 reported in literature and measured in this work (two commercially available ITO is placed for comparison; § and δ represents Lumtec and Delta samples, respectively).

treatments, *i)* contribution of O_2 plasma exposure on the electrical, optical and morphological properties of PEDOT-PSS films was systematically investigated, *ii)* in order to benefit from the superior properties of graphene while avoiding the insulator feature of GO and poor dispersion stability of rGO, Amine-modified graphene oxides (mGOs) were synthesized and used as dopants in PH1000 films and *iii)* prepared films were utilized as anodes in solution processed blue emitting OLEDs with the device structure of Glass/anode/Al4083($\cong$40 nm)/ADS231BE ($\cong$60 nm)/Cs_2CO_3(3 nm)/Al (100 nm).

2. Experimental section and methods

2.1. Materials

Poly(3,4-ethylenedioxythiophene)-poly(styrenesulfonate) (PEDOT:PSS), (Al4083) and conductive form of PEDOT:PSS (PH1000) were purchased from Clevios. Poly[9,9-di-(2-ethylhexyl)-fluorenyl-2,7-diyl], (ADS231BE) was obtained from American Dye Source. Amine sources used in the synthesis of modified GOs (mGOs) [n-Propylamine (nPRYLA), Dipropylamine (DPRYLA) and Propanolamine (PRPOHA)], solvents [acetone, isopropyl alcohol (IPA), chlorobenzene, dimethylformamide (DMF) and ethylene glycol (EG)], acids [hydrochloric acid (HCl) and sulfuric acid (H_2SO_4)], Cesium carbonate (Cs_2CO_3) and Aluminium (Al) were from Sigma Aldrich. ITO coated glass substrates with 15 Ω/sq resistivity and > 84% transmittance (@ 550 nm) were obtained from Lumtec.

2.2. Instruments for the characterization processes

Elma Transsonic T460H ultrasonic bath and CUTE FC-10046 O_2 plasma system were used in glass substrate cleaning. Nüve EV018 Vacuum Furnace was utilized in the annealing and drying processes. Optical transmission measurements were carried out by using Analytic Jena S 600 UV Spectrophotometer. Four Point Probe (Signatone PRO4-400) was used to measure the surface resistivity of the films (at least 20 measurements from different parts of the film were performed). The surface thicknesses and morphological differences were determined by using Ambios Q1 Profilometer and Ambios Qscope 250 Model Atomic Force Microscope (AFM), respectively. All solutions and suspensions were spin coated on the substrate via Laurell WS-400B-6NPP LITE under atmospheric conditions. Cathode materials were evaporated by using a thermal evaporator integrated to MBRAUN 200B Glove Box system. The current density-voltage characteristics and electroluminescence (EL) performances of the devices were determined with a Keithley 2400 programmable power source and Hamamatsu C9920-12 system, respectively. All the devices were characterized in a glove box system under inert conditions with five parallel measurements.

2.3. Preparation of PH1000 and PH1000-Solvent films and their utilization as anodes

Glass substrates were cleaned with pure water, acetone, and iso-propyl alcohol for 15 min in an ultrasonic bath and then treated with O_2 plasma (10^{-2} mbar, 70 W) for 8 min. Conductive PEDOT:PSS (PH1000) was spin coated onto the glass substrates at 2000 rpm and annealed for 60 min at two different temperatures; 120 °C and 250 °C. The choice of 250 °C was based on thermal gravimetric analysis results of PEDOT:PSS addressing that PSS group of PEDOT:PSS starts degradation at about 250 °C, while PEDOT decomposition occurs at higher temperatures (T > 350 °C) [36]. Acid treatment process was applied via dipping of the 250 °C annealed films into 1.5 M H_2SO_4 solution at 160 °C for 5 min. The films cooled to room temperature and rinsed several times with pure water to remove the residual acid solution and then re-annealed under vacuum at 160 °C for 30 min. In order to determine the optimum surface morphology, the prepared films were treated with O_2 plasma (at 10^{-2} mbar) with three different powers, *i.e.* 50, 70 and 90 W and three different exposure times, *i.e.* 2.0, 3.0, 4.0 and 5.0 min. Then optical, sheet resistance and morphological characterizations of the films were performed. Optical transmittance values are reported for the wavelength range of 350 and 750 nm in order to simulate visible region and wavelengths of 420 nm and 555 nm those of which correspond to the EL maximum of the blue OLED studied in this manuscript and the maximum spectral sensitivity of the human eye under daylight conditions, respectively. Sheet resistance values are calculated for 90% reliability.

Prepared PH1000 films were utilized as anode in the blue OLED. Al4083 was spin coated onto the anode at 3000 rpm and dried at 100 °C for 30 min ADS231BE solution in chlorobenzene (10 mg/ml) was spin-coated on Al4083 layer at 2500 rpm and annealed at 65 °C for 15 min Cs_2CO_3 and Al were vacuum evaporated onto the active layer respectively, at 2×10^{-6} mbar. The highest device performances were obtained with the device which the H_2SO_4 treated anode layer was exposed to O_2 plasma at 70 W for 3 min. Therefore, this treatment process is applied to the films, solvent effects of which were investigated. PH1000 was mixed with three different solvents (DMF, EG and IPA) in 15:1 vol ratio (v/v) and then used as anode in the blue OLED.

2.4. Synthesis of mGO derivatives

Graphene Oxide (GO) was synthesized according to the modified Hummers' method as described in our previous study [37,38]. 10 mmol of amine sources were added to 100 ml GO (2 mg/ml) dispersion and amine modification reaction was carried out at 95 °C for 24 h. The alkaline reaction solution was filtered by washing with the pure water-ethanol mixture (with 1:1 vol ratio) until the reaction medium was neutralized. This filtered solid material was dried at 70 °C for 24 h and obtained amine modified graphene oxide samples were referred as mGO. n-nPRYLA, DPRYLA and PRPOHA were used as amine sources during the GO modification and obtained mGO derivatives were called nPRYLA-GO, DPRYLA-GO and PRPOHA-GO, respectively.
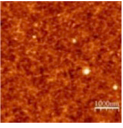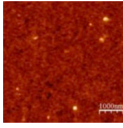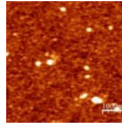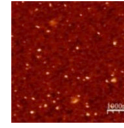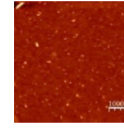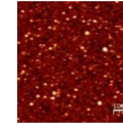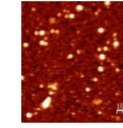
2.5. Preparation of PH1000-mGO composite films and their utilization as anode

nPRYLA-GO, DPRYLA-GO and PRPOHA-GO were utilized as dopant materials in PH1000. PH1000 was blended with mGO dispersions (2 mg/ml; in DMF, EG, and iPA) in 15:1 v/v ratio, and sonicated for ~15 min. Corresponding composites were named as PH1000:nPRYLA-GO, PH1000:DPRYLA-GO and PH1000:PRPOHA-GO. Preparation of the films was carried out as described above and optimized treatment process was also applied. Obtained films were used as anode in the blue OLED. Device fabrication procedure described in section 2.3 was repeated with the composite anodes.

The active area of all devices was 6 mm^2 and ITO anode was used as the main reference. Presented results represent the maximum

Table 1

AFM images, surface roughness (nm), surface resistivity (kΩ/sq), film thickness (nm) and optical transmittance (T%) values of thermally, H_2SO_4 and O_2 plasma treated PH1000 films.

Parameter	Annealing Temperature						
	120 °C	250 °C					
	H_2SO_4 Treatment						
	–	–	+	+	+	+	+
	O_2 plasma (70 W) time (min)						
	0	0	0	2.0	3.0	4.0	5.0
AFMImages							
RMS (nm)	2.1	2.1	3.6	6.6	6.3	8.9	12.7
Surface Resistivity (kΩ/sq)	232.6 ± 4.1	43.2 ± 0.6	0.136 ± 0.003	0.169 ± 0.002	0.252 ± 0.007	0.327 ± 0.005	0.508 ± 0.007
Thickness (nm)	106	104	68	48	40	33	28
%T (420 nm)	90.56	90.85	92.18	94.56	95.04	96.55	97.42
%T (555 nm)	90.21	90.29	92.67	94.66	95.81	96.37	97.86
%T (350–750 nm)	89.72	89.49	92.56	95.12	95.70	95.80	97.41

performances obtained from four parallel devices.

3. Results and discussion

AFM phase images, film thicknesses, surface roughness (RMS), resistivity and optical transmittance values of the PH1000 films after thermal annealing, H_2SO_4 and O_2 plasma (70 W) treatment processes are given in Table 1. Thermal treatment did not cause a remarkable change on the optical and morphological properties of the films whereas surface resistivity values were reduced ~5 folds. This is attributed to conformational changes of the PEDOT chains due to the phase segregation between the PEDOT and PSS [1] and degradation of PSS [36]. Application of H_2SO_4 treatment on the film annealed at 250 °C, resulted in a significant decrease in surface resistivity (0.136 kΩ/sq). This is explained by the interaction of H^+ and HSO_4^- ions of H_2SO_4 with PSS and PEDOT chains and formation of water soluble PSSH [23]. The film thicknesses are decreased with the rinsing off of PSSH groups from the surface by water and this resulted in a slight increase in optical transmittance.

O_2 plasma was applied on the films those of which were annealed at 250 °C and entreated with H_2SO_4. Increasing the O_2 plasma power caused a decrease in optical transparency and an increase in resistivity

Fig. 2. Deviation of surface resistivity and optical transmittance (%) of PH1000 films for the wavelength range of 350–750 nm (visible field response) depending on the applied O_2 plasma time and power.

(Fig. 2). A significant decrement in the film thickness is observed as the O_2 plasma exposure time is increased. In literature, thickness changes are addressed to occur as a result of the interaction of O_2 plasma with PSS rather than the PEDOT regions [39]. However, increasing surface resistivity values and decreasing film thicknesses show that O_2 plasma may influence the positively charged PEDOT chains as well. Although a reduction in transmittance accompanying to the increase in surface roughness was expected [40], transmittance values are increased with the O_2 exposure time. This is attributed to the dramatic decrease monitored in film thicknesses (Table 1, Fig. 2 and Fig. S1).

Depending on the O_2 plasma exposure time, the device performances of 50 and 90 W of O_2 plasma applied devices were either lower or comparable with the ITO anode (Figs. S2 and S3) whereas, 70 W of O_2 plasma applied ones presented better performances (Fig. 3). Different device performances obtained with different O_2 power exposures can be explained by the intensity of O_2 interaction with the PSS rings [39] and film thickness and resistivity deviations [11,12,14]. It is thought that optimum film thickness and surface resistivity values that are necessary for the charge carrier injection and the emission are obtained with the 70 W of O_2 plasma treatments.

PH1000 based devices presented lower current density at constant potential and better color purity with approximately 20 nm lower full width at half maximum (FWHM) values compared to that of the ITO based one. Additionally, color shifts observed depending on the applied potential with O_2 plasma treated anodes were lower compared to that of O_2 plasma untreated one (Fig. S4). Although the maximum luminance values obtained with PH1000 anodes were lower than that of the reference ITO, the efficiency values presented ≅2 fold increments. This can be attributed to weak microcavity effect that occurs due to better refractive index match between PEDOT:PSS and glass substrate compared to that of ITO and glass substrate [2,23] and enhanced compatibility between anode and HTL layer. When the maximum efficiencies achieved with the PH1000 anode exposed to 3 min of O_2 plasma are compared to the unexposed device, more than 10% of enhancement is obtained. This improvement can be attributed to the work function rising due to the dipoles on the film surface that occur by the O_2 plasma effects [41,42]. Moreover, the device with the PH1000 anode exposed to 3 min of O_2 plasma exhibited leakage current approximately one order magnitude lower than the others. It is thought that leakage current was minimized for this anode by inhibition of the capacitance effects due to its owned optimum surface resistivity, surface roughness,
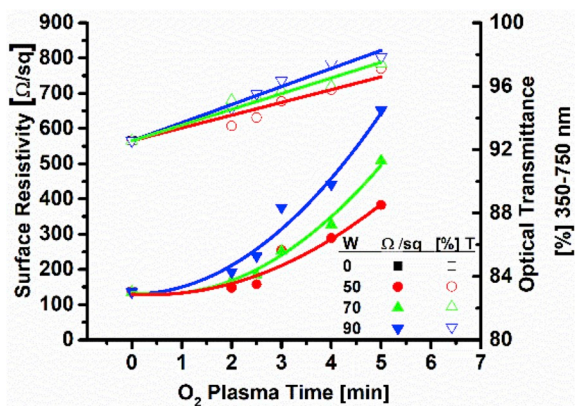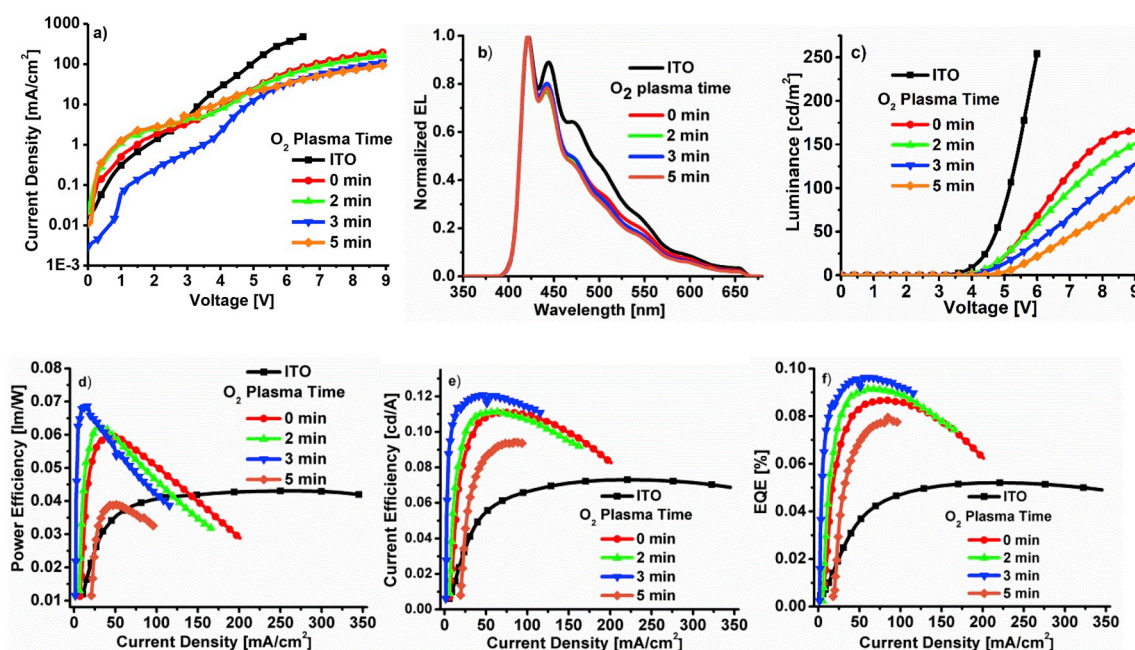
Fig. 3. Performance curves of a) Current density-voltage, b) normalized EL, c) luminance-voltage, d) power efficiency-, e) current efficiency-, f) EQE-current density of H_2SO_4 and 70 W O_2 plasma treated PH1000 anode based OLEDs with PH1000/Al4083/ADS231BE/Cs2CO3/Al device structure.

and thickness values. Although leakage current has been associated with the surface roughness dominantly in the literature, it was determined in this study that the combination of all surface properties play a key role in leakage current [43–45].

Film formation properties of H_2SO_4 and O_2 plasma treated (70W for 3 min) PH1000-solvent films are summarized in Table 2. It is known that surface resistivity and morphological properties of films strongly depend on the solvent properties such as dipole moment, boiling point and doping weight% of the solvent in PEDOT:PSS [11–13,46,47]. Contrary to the report of Thomas et al., no significant deviation was detected in the thickness values ($\pm$ 2 nm) and the roughnesses were decreased with the addition of solvents [46]. In this work, the interaction between PEDOT and PSS and the population of PSS groups were substantially reduced by both H_2SO_4 and O_2 plasma treatments. Therefore, solvents are allowed to affect mainly on PEDOT chains and the vertical charge transfer was favored by the elongation of the π-conjugation in PEDOT ring [1]. As a result, compared to the solvent-free PH1000 film, the roughness and surface resistivity of PH1000-solvent films are reduced.

When the roughnesses of films are compared depending on the dipole moment (D) and surface tension (γ) of the doped solvents, the result was as expected; surface roughnesses were decreasing as D and γ of solvent decrease (order of D and γ of solvents are DMF > EG > IPA [48]). However, this systematic change is not valid for the surface resistivity; IPA doped PH1000 film presented the lowest resistivity. It is thought that being a polar protonated solvent, IPA stabilized the PEDOT with its isoproxide part and increased the bipolaron concentration.

Compared to the solvent-free PH1000 based devices, a reduction in FWHM values was detected with PH1000-solvent anodes (Fig. S5). The charge accumulation and current leakage effects observed between 3.5 V and 5.0 V with the solvent free PH1000 and PH1000-IPA anodes were not detected with PH1000-EG and –DMF ones. PH1000-EG anode presented higher luminance and power efficiency than that of and comparable current and external quantum efficiency (EQE) values with the solvent free PH1000 device.
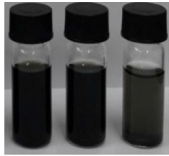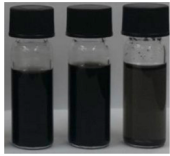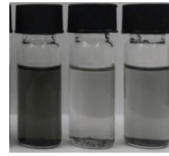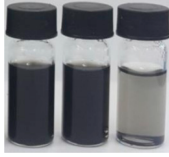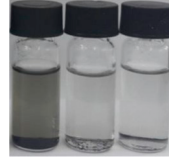
The mGO derivatives were prepared from primary (n-PRYLA), secondary (DPRYLA) and alcohol (PRPOHA) amine derivatives. Structural characterization results of mGO derivatives and the deviations observed in surface resistivity and transparency values of PH1000:mGO films prepared from DMF, EG and IPA are presented in SI (Tables S1–S4 and Figs. S6 and S7). In all cases, presence of mGO derivatives in PH1000 slightly decreased the transparency of the film and except the

Table 2

AFM images, surface roughness (nm), surface resistivity (kΩ/sq), film thickness (nm) and optical transmittance (T%) values of PH1000 and PH1000:solvents (*mixing ratio: 15:1; v:v*) films.

Parameters	PH1000	PH1000-DMF	PH1000-EG	PH1000-IPA
AFM Images				
RMS (nm)	6.3	3.7	3.0	2.4
Surface Resistivity (kΩ/sq)	0.252 ± 0.007	0.162 ± 0.014	0.214 ± 0.010	0.146 ± 0.004
Thickness (nm)	40	41	42	38
%T (420 nm)	95.04	96.53	96.12	95.53
%T (555 nm)	95.81	95.47	95.73	95.70
%T (350–750 nm)	95.70	95.14	95.29	95.16

Table 3

5 min later and 1 week later dispersion images of mGOs in different solvents.

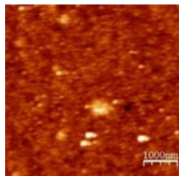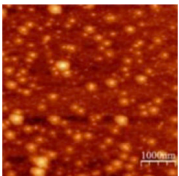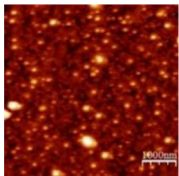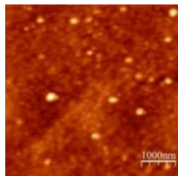| Duration	Solvents		
	DMF	EG	iPA
5 Minutes Later			
1 Week Later			
	nPRYLA-GO DPRYLA-GO PRPOHA-GO	nPRYLA-GO DPRYLA-GO PRPOHA-GO	nPRYLA-GO DPRYLA-GO PRPOHA-GO

PH1000:mGO films prepared from EG, the surface resistivities were slightly increased compared to that of their own references. Moreover, mGO derivatives presented higher dispersion stability in this solvent (Table 3 and Table S4). This observation is attributed to better interaction between the oxygenated functional groups of mGO derivatives and EG which is favored by the higher total of polar (δp) and hydrogen bond (δh) strength of EG [$(\delta p + \delta h)^{EG}$ = 37.00 MPa$^{1/2}$] than that of DMF [$(\delta p + \delta h)^{DMF}$ = 25.00 MPa$^{1/2}$] and IPA [$(\delta p + \delta h)^{IPA}$ = 22.50 MPa$^{1/2}$] [48]. Therefore, further investigation on the film properties and preparation of the ITO free devices were implemented from EG as solvent.

Surface and optical properties of PH1000:mGO (@EG) films are summarized in Table 4. The surface roughness of PH1000:mGO (@EG) films were increased compared to that of PH1000-EG reference film. It is known that GO may interact with both PEDOT and PSS chains and break the columbic attraction between them [32,49,50]. It is believed that the structural differences between the mGO derivatives affected on not only the degree of this interaction but also the degree of O_2 plasma influence on the film. Lower surface resistivity measured with PH1000:mGO films was attributed to favored separation of PEDOT from PSS, formation of PSSH species and controlled O_2 plasma effects in the presence of mGOs. The lowest surface resistivity was obtained with the PH1000:PRPOHA-GO film as alcohol amines contain acidic proton. Except the PH1000:PRPOHA-GO film, the roughness of PH1000:mGO films was much higher than that of the reference. This is due to the possible stabilization of positively charged PEDOT ring with propoxide

and higher hydrophobicity of GO derivatives that have alkyl chains (Fig. S7c). Presence of all mGO derivatives in PH1000, reduced the O_2 plasma effects on film thickness and resulted in thicker films compared to their reference. When evaluated with the decreasing surface resistivity, these results may address that mGO derivatives inhibited the reaction between the reactive oxygen species and PEDOT rings addressed in literature [51,52] and allowed the protection of conjugation.

The performance curves of the devices which contain PH1000:mGO (@EG) as anode are given in Fig. 4 in comparison with ITO, optimized PH1000 and PH1000-EG anodes. The devices with PH1000-EG and PH1000:nPRYLA-GO anodes presented overlapped EL curves. Whereas, the device with PH1000:PRPOHA-GO anode showed further decrement of 5 nm in the FWHM value. The turn on voltages ($V_{turn-on}$ is the voltage at which 1 cd/m^2 of brightness is achieved) of the devices are measured as 3.3 V, 4.5 V, 3.9 V, 4.4 V, 4.1 V and 3.7 V for ITO, PH1000, PH1000-EG, PH1000:nPRYLA-GO, PH1000:DPRYLA-GO and PH1000:PRPOHA-GO anodes, respectively. Efficiency values of all PH1000:mGO anodes presented lower values compared to PH1000 and PH1000-EG anodes but efficiency roll-off (large drop in efficiency at high brightness) observed with the applied current in PH1000 and PH1000-EG anodes was also inhibited to some extent. Reduced FWHM, $V_{turn-on}$ and efficiency roll-offs suggest that with PH1000:PRPOHA-GO anode, the barrier between the PH1000 electrode and Al4083 is reduced and a broader emission zone in the EML is provided by the stimulated hole injection [53]. When compared with ITO anode, PH1000:PRPOHA-GO presented 1.6, 1.5 and 1.9 fold enhancements in

Table 4

AFM images, surface roughness (nm), surface resistivity (kΩ/sq), film thickness (nm) and optical transmittance (T%) values of PH1000-EG and PH1000:mGOs (@ EG) films.

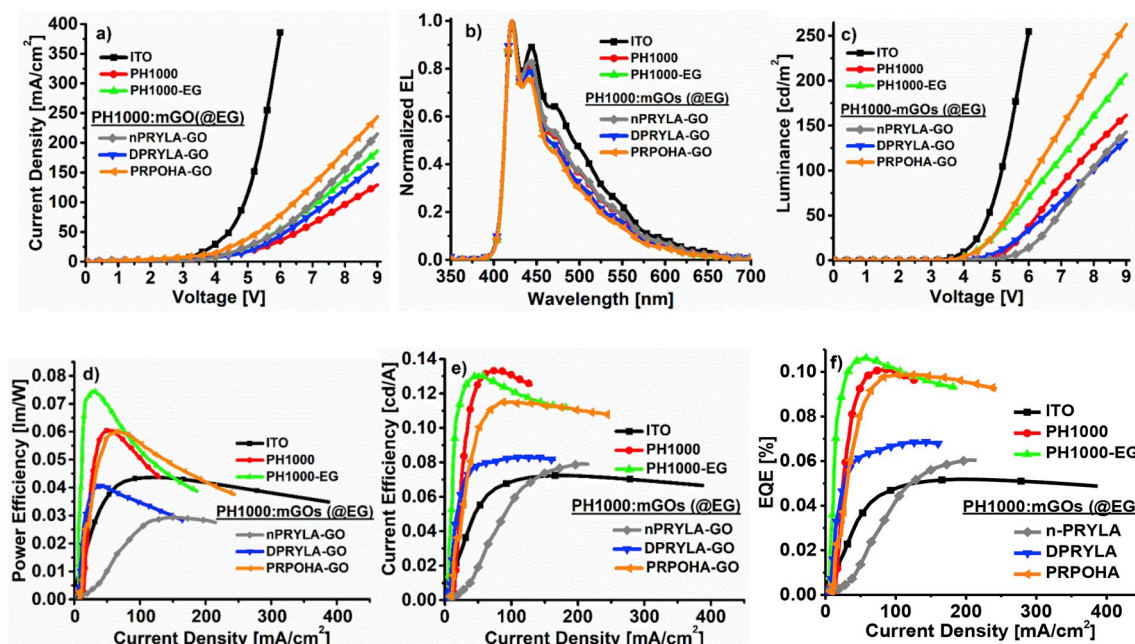| Parameter	Ethylene Glycol (EG)			
	PH1000	PH1000: nPRYLA-GO	PH1000: DPRYLA-GO	PH1000: PRPOHA-GO
AFM Images				
RMS (nm)	3.0	13.5	6.6	3.8
Surface Resistivity (kΩ/sq)	0.214 ± 0.010	0.182 ± 0.007	0.183 ± 0.006	0.177 ± 0.004
Thickness (nm)	42	44	46	50
%T (420 nm)	96.12	94.45	94.20	93.60
%T (555 nm)	95.73	94.15	94.74	93.18
%T (350–750 nm)	95.29	93.53	94.14	92.65

Fig. 4. Performance curves of **a)** Current density-voltage, **b)** normalized EL, **c)** luminance-voltage, **d)** power efficiency-, **e)** current efficiency-, **f)** EQE-current density of mGO doped PH1000 anode based OLEDs in comparison with the ones contain ITO, bare PH1000 and PH1000-EG anodes.

current and power efficiency and EQE values, respectively.

To the best of our knowledge this study represents the first report that introduce, *i)* the influence of separately followed, thermal, H_2SO_4, solvent and O_2 plasma treatments on the film formation properties of PH1000 systematically, *ii)* further contribution of mGOs synthesized with comparable chemical structures on optimized PH1000 film properties and *iii)* their performance as anodes in solution proseeced blue emitting OLED.

4. Conclusion

Application of known thermal annealing and H_2SO_4 treatments on PH1000 film resulted in a dramatic decrease in surface resistivity values; from 232.6 ± 4.1 kΩ/sq to 0.136 ± 0.003 kΩ/sq. O_2 plasma exposure applied on this film, increased the resistivity to some extent (0.252 ± 0.007 kΩ/sq), decreased the thickness and increased the transparency depending on the duration. The best device performance is achieved with the anode exposed to O_2 plasma with the power of 70W and for the duration 3 min. Application of thermal annealing, H_2SO_4 treatment and O_2 exposure to the films prepared by solvent (DMF, EG and IPA) doping in PH1000, resulted in reduced resisitivities and PH1000-EG anode presented better device efficiency than that of the solvent free PH1000 one. Synthesized, primary (n-PRYLA), secondary (DPRYLA) and alcohol (PRPOHA) amine mGOs presented better dispersion stability in EG. PH1000:mGO films presented optical transparency values higher than 90% for the wavelength range of 350–750 nm and lower resistivity (177–186 Ω/sq) compared to the PH1000-EG film (214 Ω/sq). The PH1000:PRPOHA-GO anode, presented more than 30 nm of decrement in FWHM and more than 1.5 fold enhancement in the efficiency of solution processed blue OLED, compared to that of ITO anode based device.

Supporting information

The Supporting Information contains, structural characterization results of all mGO derivatives, additional graphics for the thin film properties of PH1000 anodes and also OLED device performances (PDF).

Notes

Author Contributions: First and second authors contribute equally to the manuscript. The manuscript was written through contributions of all authors. All authors gave approval to the final version of the manuscript. The authors declare no competing financial interests.

Acknowledgment

This work was supported by the research project funds of Scientific and Technological Research Council of Turkey (TUBITAK) (Project #: 114M508).

Appendix A. Supplementary data

Supplementary data to this article can be found online at https://doi.org/10.1016/j.cap.2019.04.018.

References

[1] K. Ellmer, Past achievements and future challenges in the development of optically transparent electrodes, Nat. Photon. 6 (2012) 809–817, https://doi.org/10.1038/nphoton.2012.282.
[2] Y.H. Kim, J. Lee, S. Hofmann, M.C. Gather, L. Müller-Meskamp, K. Leo, Achieving high efficiency and improved stability in ITO-free transparent organic light-emitting diodes with conductive polymer electrodes, Adv. Funct. Mater. 23 (2013) 3763–3769, https://doi.org/10.1002/adfm.201203449.
[3] M.H. Yousefi, A. Fallahzadeh, J. Saghaei, M.D. Darareh, Fabrication of flexible ITO-Free OLED using vapor-treated PEDOT:PSS thin film as anode, J. Disp. Technol. 12 (2016) 1647–1651, https://doi.org/10.1109/JDT.2016.2624341.
[4] C.M. Aguirre, S. Auvray, S. Pigeon, R. Izquierdo, P. Desjardins, R. Martel, Carbon nanotube sheets as electrodes in organic light-emitting diodes, Appl. Phys. Lett. 88 (2006), https://doi.org/10.1063/1.2199461.
[5] Y. Zhou, S. Shimada, T. Saito, R. Azumi, Building interconnects in carbon nanotube networks with metal halides for transparent electrodes, Carbon N. Y. 87 (2015) 61–69, https://doi.org/10.1016/j.carbon.2015.01.031.
[6] J. Lee, T.H. Han, M.H. Park, D.Y. Jung, J. Seo, H.K. Seo, et al., Synergetic electrode architecture for efficient graphene-based flexible organic light-emitting diodes, Nat. Commun. 7 (2016) 1–9, https://doi.org/10.1038/ncomms11791.
[7] S. Jia, H.D. Sun, J.H. Du, Z.K. Zhang, D.D. Zhang, L.P. Ma, et al., Graphene oxide/graphene vertical heterostructure electrodes for highly efficient and flexible organic light emitting diodes, Nanoscale 8 (2016) 10714–10723, https://doi.org/10.1039/c6nr01649a.
[8] L. Shi, J. Yang, T. Yang, Q. Hanxun, Q. Zheng, Molecular level controlled

915

fabrication of highly transparent conductive reduced graphene oxide/silver nanowire hybrid films, RSC Adv. 4 (2014) 43270–43277, https://doi.org/10.1039/C4RA07228F.

[9] C. Sachse, L. Müller-Meskamp, L. Bormann, Y.H. Kim, F. Lehnert, A. Philipp, et al., Transparent, dip-coated silver nanowire electrodes for small molecule organic solar cells, Org. Electron. 14 (2013) 143–148, https://doi.org/10.1016/j.orgel.2012.09.032.

[10] Y.H. Kim, L. Müller-Meskamp, K. Leo, Ultratransparent polymer/semitransparent silver grid hybrid electrodes for small-molecule organic solar cells, Adv. Energy Mater. 1401822 (2015) 1–5, https://doi.org/10.1002/aenm.201401822.

[11] Y.K. Seo, J.W. Han, K.T. Lim, Y.H. Kim, C.W. Joo, J. Lee, et al., Efficient ITO-free organic light-emitting diodes comprising PEDOT:PSS transparent electrodes optimized with 2-ethoxyethanol and post treatment, Org. Electron. 42 (2017) 348–354, https://doi.org/10.1016/j.orgel.2016.12.059.

[12] Y.K. Seo, C.W. Joo, J. Lee, J.W. Han, D.J. Lee, S.A.N. Entifar, et al., Enhanced electrical properties of PEDOT:PSS films using solvent treatment and its application to ITO-free organic light-emitting diodes, J. Lumin. 187 (2017) 221–226, https://doi.org/10.1016/j.jlumin.2017.03.002.

[13] J. Nevrela, M. Micjan, M. Novota, S. Kovacova, M. Pavuk, P. Juhasz, et al., Secondary doping in poly(3,4-ethylenedioxythiophene):Poly(4-styrenesulfonate) thin films, J. Polym. Sci., Part B: Polym. Phys. 53 (2015) 1139–1146, https://doi.org/10.1007/978-94-007-7587-9_2.

[14] X. Crispin, F.L.E. Jakobsson, A. Crispin, P.C.M. Grim, P. Andersson, A. Volodin, et al., The origin of the high conductivity of poly(3,4-ethylenedioxythiophene)−poly(styrenesulfonate) (PEDOT−PSS) plastic electrodes, Chem. Mater. 18 (2006) 4354–4360, https://doi.org/10.1021/cm061032+.

[15] Y. Zhang, Z. Wu, P. Li, L.K. Ono, Y. Qi, J. Zhou, et al., Fully solution-processed TCO-free semitransparent perovskite solar cells for tandem and flexible applications, Adv. Energy Mater. 8 (2018) 1–10, https://doi.org/10.1002/aenm.201701569.

[16] B. Fan, X. Mei, J. Ouyang, Significant conductivity enhancement of conductive poly(3,4-ethylenedioxythiophene):poly(styrenesulfonate) films by adding anionic surfactants into polymer solution, Macromolecules 41 (2008) 5971–5973, https://doi.org/10.1021/ma8012459.

[17] C. Badre, L. Marquant, A.M. Alsayed, L.A. Hough, Highly conductive poly(3,4-ethylenedioxythiophene):Poly (styrenesulfonate) films using 1-ethyl-3-methylimidazolium tetracyanoborate ionic liquid, Adv. Funct. Mater. 22 (2012) 2723–2727, https://doi.org/10.1002/adfm.201200225.

[18] Y. Xia, J. Ouyang, PEDOT:PSS films with significantly enhanced conductivities induced by preferential solvation with cosolvents and their application in polymer photovoltaic cells, J. Mater. Chem. 21 (2011) 4927–4936, https://doi.org/10.1039/c0jm04177g.

[19] Q. Wang, M. Eslamian, Improving uniformity and nanostructure of solution-processed thin films using ultrasonic substrate vibration post treatment (SVPT), Ultrasonics 67 (2016) 55–64, https://doi.org/10.1016/j.ultras.2015.12.012.

[20] Q. Wang, M.R. Ahmadian-Yazdi, M. Eslamian, Investigation of morphology and physical properties of modified PEDOT: PSS films made via in-situ grafting method, Synth. Met. 209 (2015) 521–527, https://doi.org/10.1016/j.synthmet.2015.09.003.

[21] Y. Xia, J. Ouyang, Significant conductivity enhancement of conductive poly(3,4-ethylenedioxythiophene): poly(styrenesulfonate) films through a treatment with organic carboxylic acids and inorganic acids, ACS Appl. Mater. Interfaces 2 (2010) 474–483, https://doi.org/10.1021/am900708x.

[22] Y.F. Liu, J. Feng, Y.F. Zhang, H.F. Cui, D. Yin, Y.G. Bi, et al., Improved efficiency of indium-tin-oxide-free flexible organic light-emitting diodes, Org. Electron. 15 (2014) 478–483, https://doi.org/10.1016/j.orgel.2013.11.035.

[23] M. Cai, Z. Ye, T. Xiao, R. Liu, Y. Chen, R.W.R.W. Mayer, et al., Extremely efficient indium-tin-oxide-free green phosphorescent organic light-emitting diodes, Adv. Mater. 24 (2012) 4337–4342, https://doi.org/10.1002/adma.201202035.

[24] D. Alemu, H.Y. Wei, K.C. Ho, C.W. Chu, Highly conductive PEDOT:PSS electrode by simple film treatment with methanol for ITO-free polymer solar cells, Energy Environ. Sci. 5 (2012) 9662–9671, https://doi.org/10.1039/c2ee22595f.

[25] N. Kim, S. Kee, S.H. Lee, B.H. Lee, Y.H. Kahng, Y.R. Jo, et al., Highly conductive PEDOT:PSS nanofibrils induced by solution-processed crystallization, Adv. Mater. 26 (2014) 2268–2272, https://doi.org/10.1002/adma.201304611.

[26] S. Park, C.W. Lee, J.M. Kim, Highly conductive PEDOT:PSS patterns based on photo-crosslinkable and water-soluble diacetylene diol additives, Org. Electron. 58 (2018) 1–5, https://doi.org/10.1016/j.orgel.2018.03.044.

[27] Z. Zhao, Q. Liu, W. Zhang, S. Yang, Conductivity enhancement of PEDOT:PSS film via sulfonic acid modification: application as transparent electrode for ITO-free polymer solar cells, Sci. China Chem. 61 (2018) 1179–1186, https://doi.org/10.1007/s11426-017-9205-x.

[28] B. Vaagensmith, K.M. Reza, M.D.N. Hasan, H. Elbohy, N. Adhikari, A. Dubey, et al., Environmentally friendly plasma-treated PEDOT:PSS as electrodes for ITO-free perovskite solar cells, ACS Appl. Mater. Interfaces 9 (2017) 35861–35870, https://doi.org/10.1021/acsami.7b10987.

[29] Y.-F. Liu, J. Feng, Y.-F. Zhang, H.-F. Cui, D. Yin, Y.-G. Bi, et al., Improved efficiency of indium-tin-oxide-free organic light-emitting devices using PEDOT:PSS/graphene oxide composite anode, Org. Electron. 26 (2015) 81–85, https://doi.org/10.1016/j.orgel.2015.06.031.

[30] X. Wu, J. Liu, Y. Wang, Z. Min, M. Yang, G. He, Highly conductive graphene and PEDOT: PSS hybrid film with the treatment by hydroiodic acid for indium tin

oxide-free flexible organic light emitting diodes, Soc. Inf. Disp. (2015) 1654–1657, https://doi.org/10.1002/sdtp.10150.

[31] H. Chang, G. Wang, A. Yang, X. Tao, X. Liu, Y. Shen, et al., A transparent, flexible, low-temperature, and solution-processible graphene composite electrode, Adv. Funct. Mater. 20 (2010) 2893–2902, https://doi.org/10.1002/adfm.201000900.

[32] X. Wu, J. Liu, D. Wu, Y. Zhao, X. Shi, J. Wang, et al., Highly conductive and uniform graphene oxide modified PEDOT:PSS electrodes for ITO-Free organic light emitting diodes, J. Mater. Chem. C. 2 (2014) 4044–4050, https://doi.org/10.1039/c4tc00305e.

[33] X. Wu, L. Lian, S. Yang, G. He, Highly conductive PEDOT:PSS and graphene oxide hybrid film with the dipping treatment by hydroiodic acid for organic light emitting diodes, J. Mater. Chem. C. 4 (2016) 8528–8534, https://doi.org/10.1039/c6tc02424f.

[34] Y.G. Seol, T.Q. Trung, O.J. Yoon, I.Y. Sohn, N.E. Lee, Nanocomposites of reduced graphene oxide nanosheets and conducting polymer for stretchable transparent conducting electrodes, J. Mater. Chem. 22 (2012) 23759–23766, https://doi.org/10.1039/c2jm33949h.

[35] X. Hu, X. Meng, J. Xiong, Z. Huang, X. Yang, L. Tan, et al., Roll-to-Roll fabrication of flexible orientated graphene transparent electrodes by shear Force and one-step reducing post-treatment, Adv. Mater. Technol. 2 (2017) 1–8, https://doi.org/10.1002/admt.201700138.

[36] A. Elschner, S. Kirchmeyer, W. Lövenich, U. Merker, K. Reuter, PEDOT: Principles and Applications of an Intrinsically Conductive Polyme, first ed., CRC Press, Boca Raton, 2010, https://doi.org/10.1201/b10318.

[37] W.S. Hummers, R.E. Offeman, Preparation of graphitic oxide, J. Am. Chem. Soc. 80 (1958) 1339, https://doi.org/10.1021/ja01539a017.

[38] H. Diker, G.B. Durmaz, H. Bozkurt, F. Yeşil, C. Varlikli, Controlling the distribution of oxygen functionalities on GO and utilization of PEDOT:PSS-GO composite as hole injection layer of a solution processed blue OLED, Curr. Appl. Phys. 17 (2017), https://doi.org/10.1016/j.cap.2017.02.002.

[39] Y. Zhou, Y. Yuan, J. Lian, J. Zhang, H. Pang, L. Cao, et al., Mild oxygen plasma treated PEDOT:PSS as anode buffer layer for vacuum deposited organic light-emitting diodes, Chem. Phys. Lett. 427 (2006) 394–398, https://doi.org/10.1016/j.cplett.2006.06.035.

[40] A. Larena, F. Millan, G. Perez, G. Pinto, Effect of surface roughness on the optical properties of multilayer polymer film, Appl. Surf. Sci. 187 (2002) 339–340, https://doi.org/10.1016/S0169-4332(01)01044-3.

[41] T. Nagata, S. Oh, T. Chikyow, Y. Wakayama, Effect of UV-ozone treatment on electrical properties of PEDOT:PSS film, Org. Electron. 12 (2011) 279–284, https://doi.org/10.1016/j.orgel.2010.11.009.

[42] Z. Su, L. Wang, Y. Li, H. Zhao, B. Chu, W. Li, Ultraviolet-ozone-treated PEDOT:PSS as anode buffer layer for organic solar cells, Nanoscale Res. Lett. 7 (2012) 465, https://doi.org/10.1186/1556-276X-7-465.

[43] J.H. Lee, M.H. Wu, C.C. Chao, H.L. Chen, M.K. Leung, High efficiency and long lifetime OLED based on a metal-doped electron transport layer, Chem. Phys. Lett. 416 (2005) 234–237, https://doi.org/10.1016/j.cplett.2005.09.104.

[44] K.B. Kim, Y.H. Tak, Y.S. Han, K.H. Baik, M.H. Yoon, M.H. Lee, Relationship between surface roughness of indium tin oxide and leakage current of organic light-emitting diode, Jpn. J. Appl. Phys. 42 (2003) L438–L440, https://doi.org/10.1143/JJAP.42.L438.

[45] M.H. Lee, W.H. Choi, F. Zhu, Solution-processable organic-inorganic hybrid hole injection layer for high efficiency phosphorescent organic light-emitting diodes, Optic Express 24 (2016) A592, https://doi.org/10.1364/OE.24.00A592.

[46] J.P. Thomas, L. Zhao, D. McGillivray, K.T. Leung, High-efficiency hybrid solar cells by nanostructural modification in PEDOT:PSS with co-solvent addition, J. Mater. Chem. A. 2 (2014) 2383–2389, https://doi.org/10.1039/c3ta14590e.

[47] J.Y. Kim, J.H. Jung, D.E. Lee, J. Joo, Enhancement of electrical conductivity of poly(3,4-ethylenedioxythiophene)/poly(4-styrenesulfonate) by a change of solvents, Synth. Met. 126 (2002) 311–316, https://doi.org/10.1016/S0379-6779(01)00576-8.

[48] C.M. Hansen, Hansen Solubility Parameters A User's Handbook, (2013), https://doi.org/10.1007/CBO9781107415324.004.

[49] M.M. Islam, S.H. Aboutalebi, D. Cardillo, H.K. Liu, K. Konstantinov, S.X. Dou, Self-assembled multifunctional hybrids: toward developing high-performance graphene-based architectures for energy storage devices, ACS Cent. Sci. 1 (2015) 206–216, https://doi.org/10.1021/acscentsci.5b00189.

[50] P.G. Raj, V.S. Rani, A. Kanwat, J. Jang, Enhanced organic photovoltaic properties via structural modifications in PEDOT : PSS due to graphene oxide doping, Mater. Res. Bull. 74 (2016) 346–352, https://doi.org/10.1016/j.materresbull.2015.10.044.

[51] C.V. Amanchukwu, M. Gauthier, T.P. Batcho, C. Symister, Y. Shao-Horn, J.M. D'Arcy, et al., Evaluation and stability of PEDOT polymer electrodes for Li-O2 batteries, J. Phys. Chem. Lett. 7 (2016) 3770–3775, https://doi.org/10.1021/acs.jpclett.6b01986.

[52] E. Mitraka, M.J. Jafari, M. Vagin, X. Liu, M. Fahlman, T. Ederth, et al., Oxygen-induced doping on reduced PEDOT, J. Mater. Chem. A. 5 (2017) 4404–4412, https://doi.org/10.1039/c6ta10521a.

[53] G. Liaptsis, K. Meerholz, Crosslinkable TAPC-based hole-transport materials for solution-processed organic light-emitting diodes with reduced efficiency roll-off, Adv. Funct. Mater. 23 (2013) 359–365, https://doi.org/10.1002/adfm.201201197.